

# Topological insulators for high performance terahertz to infrared applications

Xiao Zhang,<sup>1</sup> Jing Wang,<sup>2</sup> and Shou-Cheng Zhang<sup>3</sup>

<sup>1</sup>*Department of Electrical Engineering, Stanford University, Stanford, CA 94305, USA*

<sup>2</sup>*Department of Physics, Tsinghua University, Beijing 100084, China*

<sup>3</sup>*Department of Physics, McCullough Building, Stanford University, Stanford, CA 94305-4045*

(Dated: October 29, 2018)

Topological insulators in the  $\text{Bi}_2\text{Se}_3$  family have an energy gap in the bulk and a gapless surface state consisting of a single Dirac cone. Low frequency optical absorption due to the surface state is universally determined by the fine structure constant. When the thickness of these three dimensional topological insulators is reduced, they become quasi-two dimensional insulators with enhanced absorbance. The two dimensional insulators can be topologically trivial or non-trivial depending on the thickness, and we predict that the optical absorption is larger for topological non-trivial case compared with the trivial case. Since the three dimensional topological insulator surface state is intrinsically gapless, we propose its potential application in wide bandwidth, high performance photo-detection covering a broad spectrum ranging from terahertz to infrared. The performance of photodetection can be dramatically enhanced when the thickness is reduced to several quintuple layers, with a widely tunable band gap depending on the thickness.

PACS numbers: 78.68.+m 78.20.Bh, 78.20.Ci, 78.56.-a

Topological insulators (TIs) are a new state of quantum matter with an insulating bulk gap and gapless edge or surface states interesting for condensed matter physics, material science and electrical engineering<sup>1-8</sup>. The two-dimensional (2D) TI, with quantum spin Hall (QSH) effect has been predicted and observed in  $\text{HgTe}/\text{CdTe}$  quantum well<sup>2,3</sup>. Recently, 3D TI such as  $\text{Bi}_2\text{Se}_3$  and  $\text{Bi}_2\text{Te}_3$  were theoretically predicted to have bulk energy gap as large as 0.3eV, and gapless surface states consisting of a single Dirac cone<sup>6,7</sup>. The angle-resolved photoemission spectroscopy (ARPES) observed such linear Dirac spectrum dispersing from the  $\Gamma$  point in both of these materials<sup>7,8</sup>.  $\text{Bi}_2\text{Se}_3$  and  $\text{Bi}_2\text{Te}_3$  are stoichiometric rhombohedral crystals with layered structure consisting of stacked quintuple layers (QLs), with relatively weak Van der Waals coupling between QLs (each QL is about 1nm thick). Therefore high quality thin films have been successfully grown on silicon and silicon carbide substrates via molecular beam epitaxy<sup>9-11</sup>, layer by layer, which enables further scientific study and applications integratable with today's electronics. These materials have also been grown by Au-catalyzed vapor-liquid-solid<sup>12</sup> and catalyst-free vapor-solid chemical vapor deposition methods<sup>13</sup> on silicon, silicon dioxide and silicon nitride substrates. The surface states of such thin film have been predicted<sup>6,14,15</sup> and observed to open a gap when they are thinner than 6 QLs<sup>9</sup>. Up to now, few study on optical properties of the topological surface states has been reported. On the other hand, the single Dirac cone on the  $\text{Bi}_2\text{Se}_3$  surface can be imagined as 1/4 of graphene<sup>16</sup>, it is straightforward to study the optical properties and relevant applications of TI in analogy to the optoelectronics applications of graphene<sup>17-19</sup>.

Starting from an effective  $\mathbf{k} \cdot \mathbf{p}$  Hamiltonian and ignoring intra-unit cell dipole contribution to absorbance, we show that the low energy optical absorbance of thin film  $\text{Bi}_2\text{Se}_3$  thicker than 6 QLs is a universal quantity  $\pi\alpha/2$ , which does not depend on the photon energy or chemical composition of the material, where  $\alpha$  is the fine structure constant. This originates from Dirac nature of the 2D topological surface states. Furthermore, the optical transitions from the valence to con-

duction surface bands depend solely on the spin-states in contrast to the conventional semiconductors. When the thickness of such thin film is less than 6 QLs, a gap is opened up for the surface states around the  $\Gamma$  point<sup>9,14,15,20</sup>, and the resulting 2D insulator can either be topologically trivial, or non-trivial, depending the thickness of the film<sup>15</sup>. We show here that the optical absorbance near the band edge is either smaller or larger than  $\pi\alpha$ , depending on it is conventional insulator or 2D QSH insulator. This suggests an optical mean to measure its topological nature other than transport<sup>3</sup>. With such strong absorbance, the thin film  $\text{Bi}_2\text{Se}_3$  may be a promising candidate for high performance photodetector in the terahertz (THz) to infrared frequency range. The gapless 3D TI can cover this full spectrum just by a single device with high signal-to-noise ratio (SNR) comparable to multiple structures using the conventional photodetecting material - bulk  $\text{Hg}_{1-x}\text{Cd}_x\text{Te}$ <sup>21-23</sup> with different fraction  $x$ . The SNR can be further enhanced to be about 15 times better with reduced thickness of  $\text{Bi}_2\text{Se}_3$  less than 6 QLs. Graphene has been recently demonstrated as a THz photodetector<sup>18</sup>. With almost the same high absorbance<sup>17</sup>, TI photodetector proposed here has many advantages. The prominent one is a tunable surface band gap which is easily achieved by reducing the thickness, which is necessary in many optoelectronics applications<sup>24</sup>.

## I. EFFECTIVE MODEL FOR THIN FILM TI

3D TI like  $\text{Bi}_2\text{Se}_3$  is characterized by a surface state consisting of a single Dirac cone, where the spin points perpendicular to the momentum<sup>6</sup>

$$\mathcal{H}_{surf} = A_2 (k_y \sigma^x - k_x \sigma^y), \quad (1)$$

with  $A_2 = \hbar v_F$ ,  $v_F$  is the Fermi velocity and  $\sigma^{x,y}$  are Pauli matrices describing the spin. When the thickness of a film is reduced, overlapping between the surface state wave functions from the upper and lower surfaces of the film becomes non-negligible, and hybridization between them will induce a gap

at Dirac point to avoid crossing of bands<sup>20</sup>. Furthermore, the 2D energy gap is predicted to oscillate between the ordinary insulating gap and QSH gap as a function of thickness<sup>15</sup>. The effective model of the quasi-2D system can be derived from the  $\mathbf{k} \cdot \mathbf{p}$  Hamiltonian for 3D TI<sup>25</sup>,

$$\mathcal{H}_0^{3D} = \begin{pmatrix} \mathcal{M}(\mathbf{k}) & A_1 k_z & 0 & A_2 k_- \\ A_1 k_z & -\mathcal{M}(\mathbf{k}) & A_2 k_- & 0 \\ 0 & A_2 k_+ & \mathcal{M}(\mathbf{k}) & -A_1 k_z \\ A_2 k_+ & 0 & -A_1 k_z & -\mathcal{M}(\mathbf{k}) \end{pmatrix} + \epsilon_0(\mathbf{k}), \quad (2)$$

with  $k_{\pm} = k_x \pm ik_y$ ,  $\epsilon_0(\mathbf{k}) = C_0 + D_2(k_x^2 + k_y^2) + D_1 k_z^2$ ,  $\mathcal{M}(\mathbf{k}) = M_0 + B_2(k_x^2 + k_y^2) + B_1 k_z^2$ , and the four basis of the 3D Hamiltonian are denoted as  $|P1_z^+, \uparrow\rangle$ ,  $|P2_z^-, \uparrow\rangle$ ,  $|P1_z^+, \downarrow\rangle$ ,  $|P2_z^-, \downarrow\rangle$  with the superscript  $\pm$  standing for even and odd parity and  $\uparrow$  ( $\downarrow$ ) for spin up (down). When the TI film is thin,  $k_z$  is no longer a good quantum number, by replacing  $k_z \rightarrow -i\partial_z$  and with the in-plane momentum  $\mathbf{k}_{\parallel}$  good quantum numbers, then 3D model can be expressed as  $\mathcal{H}_0^{3D}(\mathbf{k}_{\parallel}, -i\partial_z) \equiv \mathcal{H}_0^{3D}(\mathbf{k}_{\parallel} = 0, -i\partial_z) + \delta\mathcal{H}_0^{3D}$ , where  $\mathcal{H}_0^{3D}(\mathbf{k}_{\parallel} = 0, -i\partial_z)$  is block diagonal and can be solved exactly, then 2D thin film model can be obtained by projecting  $\mathcal{H}_0^{3D}$  on the eigenstates of  $\mathcal{H}_0^{3D}(\mathbf{k}_{\parallel} = 0, -i\partial_z)$  (denoted as  $|1, \uparrow\rangle$ ,  $|2, \uparrow\rangle$ ,  $|1, \downarrow\rangle$ ,  $|2, \downarrow\rangle$ ),

$$\mathcal{H}_0^{2D} = \begin{pmatrix} \tilde{\mathcal{M}}(\mathbf{k}_{\parallel}) & 0 & 0 & \tilde{A}_2 k_- \\ 0 & -\tilde{\mathcal{M}}(\mathbf{k}_{\parallel}) & \tilde{A}_2 k_- & 0 \\ 0 & \tilde{A}_2 k_+ & \tilde{\mathcal{M}}(\mathbf{k}_{\parallel}) & 0 \\ \tilde{A}_2 k_+ & 0 & 0 & -\tilde{\mathcal{M}}(\mathbf{k}_{\parallel}) \end{pmatrix} + \tilde{\epsilon}_0(\mathbf{k}_{\parallel}), \quad (3)$$

it is nothing but the model of Bernevig, Hughes and Zhang (BHZ) for the 2D QSH insulator<sup>2,15,20</sup> with  $\tilde{\epsilon}_0(\mathbf{k}_{\parallel}) = \tilde{C}_0 + \tilde{D}_2(k_x^2 + k_y^2)$ ,  $\tilde{\mathcal{M}}(\mathbf{k}_{\parallel}) = \tilde{M}_0 + \tilde{B}_2(k_x^2 + k_y^2)$ , and  $\tilde{C}_0$ ,  $\tilde{D}_2$ ,  $\tilde{M}_0$ ,  $\tilde{B}_2$  and  $\tilde{A}_2$  are parameters which are thickness dependent. The energy dispersion is  $\epsilon_{\pm}(\mathbf{k}) = \tilde{\epsilon}_0(\mathbf{k}) \pm \sqrt{\tilde{A}_2^2 k_{\parallel}^2 + \tilde{\mathcal{M}}(\mathbf{k}_{\parallel})^2}$ , which is double degenerate and gives a gap of  $2|\tilde{M}_0|$  at  $\Gamma$  point. As has been experimentally demonstrated in Ref. 9, a finite surface gap is induced when the TI film of  $\text{Bi}_2\text{Se}_3$  is less than 6 QLs.

## II. OPTICAL ABSORBANCE AND SELECTION RULES

Coupling to external electromagnetic field  $\mathbf{A}$  is described by the model Hamiltonian (3), with the replacement of  $\mathbf{k}$  by  $\mathbf{k} - \frac{e}{\hbar}\mathbf{A}$ . As in the case of graphene, the massless Dirac spectrum leads to the universal optical absorbance  $\mathcal{P}_{\text{graphene}} = \pi\alpha^{17}$ . Such optical properties being defined by the fundamental constants originates from the two-dimensional nature and gapless electronic spectrum of graphene. This suggests the universal absorbance should also be true for the helical surface states of TI. When the thickness of  $\text{Bi}_2\text{Se}_3$  thin film exceeds 6 QLs, the low energy optical absorption of its gapless surfaces can always occur with photon energy ranging from 0 to 0.3eV, where the high energy cut-off is the bulk band gap. Within the dipole moment approximation, we can write down the interacting Hamiltonian due to the optical transitions from

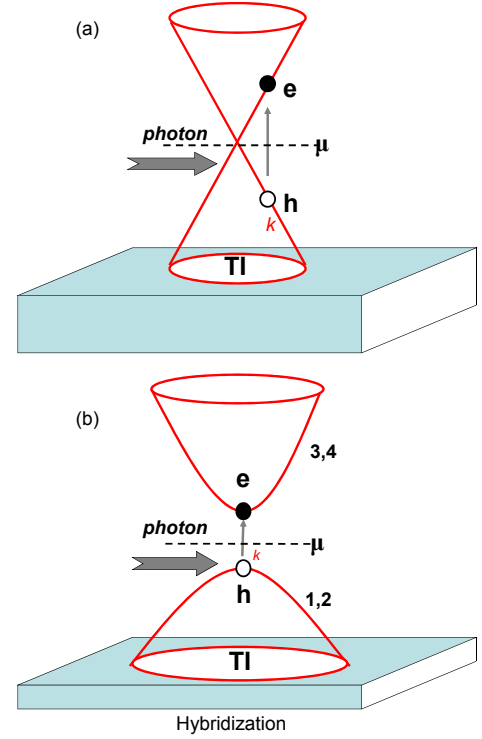


FIG. 1: **Optical absorption of surface states.** The particle and hole pair generation during photon absorption for (a) 3D and (b) 2D TI surfaces.

the the valence to conduction surface bands,

$$\begin{aligned} \mathcal{H} &= \mathcal{H}_0 + \mathcal{H}_1 \\ &= \sum_{\mathbf{k}} \left( \sum_{i=1}^4 \epsilon_{\mathbf{k},i} a_{\mathbf{k},i}^\dagger a_{\mathbf{k},i} + \frac{e}{\hbar} A_2 \mathbf{A}(t) \cdot \sum_{i,j=1}^4 a_{\mathbf{k},i}^\dagger \mathcal{D}_{ij}(\mathbf{k}) a_{\mathbf{k},j} \right), \quad (4) \end{aligned}$$

where  $a_{\mathbf{k},i}$  are the band operators with energy dispersion  $\epsilon_{1,2} = \epsilon_-$  and  $\epsilon_{3,4} = \epsilon_+$ , respectively.  $\mathbf{A}(t)$  is the vector potential.  $\mathcal{D}(\mathbf{k})$  is the interband transition operator,

$$\mathcal{D}(\mathbf{k}) = \begin{pmatrix} 0 & 0 & \hat{e}_+ & 0 \\ 0 & 0 & 0 & \hat{e}_- \\ \hat{e}_- & 0 & 0 & 0 \\ 0 & \hat{e}_+ & 0 & 0 \end{pmatrix} \quad (5)$$

where  $\hat{e}_{\pm} = \hat{e}_x \pm i\hat{e}_y$ . Here we have neglected the small wavevector of light. Taking into account the momentum conservation  $\mathbf{k}$  for the initial  $|i\rangle$  and final  $|f\rangle$  states, only the excitation processes pictured in Fig. 1(a) contribute to the light absorption. The absorption power per unit area is given by  $W_a = \Gamma \hbar \omega$ , where  $\Gamma$  is the absorption events per unit time per unit area, calculated by using Fermi's golden rule to be  $\Gamma = (2\pi/\hbar) \sum_{i,f,\mathbf{k}} | \langle f | \mathcal{H}_1 | i \rangle |^2 \delta(E_f - E_i - \hbar\omega)$ , and  $\omega$  is the optical frequency. The incident energy flux  $W_i$  is given by  $W_i = (c/4\pi) |\mathbf{A}(t)|^2 \omega^2$ . Then the absorbance is defined as the ratio of absorbed light energy flux divided by the incident light

energy flux

$$\mathcal{P}_{\text{gapless}} = \frac{W_a}{W_i} = \frac{\pi}{2}\alpha, \quad (6)$$

where  $\alpha$  is the fine structure constant. The universal optical absorption does not depend on the photon energy. For the interaction of light with relativistic helical surface states is described by a single coupling constant, i.e. the fine structure constant. The Fermi velocity is only a prefactor for both  $\mathcal{H}_0$  and  $\mathcal{H}_1$ , accordingly, one can expect that the coefficient may not change the strength of the interaction, as indeed our calculations show. When a TI film is suspended in air,  $\alpha = 1/137$  and thus  $\mathcal{P} = 1.15\%$ . It is among materials with highest absorbance, about 200 times larger than bulk  $\text{Hg}_{1-x}\text{Cd}_x\text{Te}$  of equivalent thickness, with absorption coefficient about  $100\text{cm}^{-1}$  for incident infrared light<sup>21</sup>. It is also just half of the value of a single layer graphene. This is because for 3D TI film, the up and down surfaces gives 2 gapless Dirac fermions, while for single layer graphene, the two Dirac cones together and two real spins provide a degenerate factor of 4.

As the energy gap is opened around the Dirac point in the thin film TI like  $\text{Bi}_2\text{Se}_3$  less than 6 QLs, interband real transitions between the conduction and valence surface bands can be excited by optical field when the photon energy  $\hbar\omega$  exceeds the surface band gap  $2|\tilde{M}_0|$  (Fig. 1(b)). Around the band edge

( $\mathbf{k} \rightarrow 0$ ), the transition operator is exactly the same as in the gapless case, and the absorbance is

$$\mathcal{P}_{\text{gapped}} = \pi\alpha \frac{1}{1 + 2\tilde{M}_0\tilde{B}_2/\tilde{A}_2^2}. \quad (7)$$

Thus the absorbance for the gapped surface states is around  $\pi\alpha$ , about twice higher than the gapless case. In particular, for 2 and 3QL, the absorbance is 1.8% and 2.05%, smaller than  $\pi\alpha$ , and for 4 and 5QL, the absorbance is 3.85% and 6.22%, larger than  $\pi\alpha$ . The sign of  $\tilde{M}_0\tilde{B}_2$  determines the nontrivial or trivial topology of the quasi-2D band structure<sup>2,15</sup>.  $\tilde{M}_0\tilde{B}_2 < 0$  and  $\mathcal{P}_{\text{gapped}} > \pi\alpha$ , the system is in the inverted regime, i.e. the QSH insulating states; while  $\tilde{M}_0\tilde{B}_2 > 0$  and  $\mathcal{P}_{\text{gapped}} < \pi\alpha$ , the system is just conventional insulator. This suggests an optical way to identify the topological nature other than transport measurement<sup>3</sup>.

In reality, the absorption occurs not just around band edge, so from the point of view for application, we should get the full surface absorption spectrum. Thus the transition rate is

$$\Gamma = (2\pi/\hbar) \sum_{i,f,\mathbf{k}} | \langle f | \mathcal{H}_1 | i \rangle |^2 \delta(E_f - E_i - \hbar\omega) \quad (8)$$

The absorbance is

$$\mathcal{P}_{\text{gapped}}(\omega) = \frac{\Gamma_{\text{total}}(\omega)\hbar\omega}{W_i} = \frac{\mathcal{P}_{\text{gapped}}(\tilde{M}_0)}{\sqrt{1 + \frac{\tilde{B}_2^2(\hbar^2\omega^2 - 4\tilde{M}^2)}{(\tilde{A}_2^2 + 2\tilde{M}\tilde{B}_2)^2}}} \left( 1 - \frac{\tilde{A}_2^2}{\tilde{B}_2^2} \frac{-(\tilde{A}_2^2 + 2\tilde{M}\tilde{B}_2) + \sqrt{(\tilde{A}_2^2 + 2\tilde{M}\tilde{B}_2)^2 + \tilde{B}_2^2(\hbar^2\omega^2 - 4\tilde{M}^2)}}{\hbar^2\omega^2} \right), \quad (9)$$

$\mathcal{P}_{\text{gapped}}(\tilde{M}_0)$  is the band edge absorbance and the parameters for  $\text{Bi}_2\text{Se}_3$  are in Ref. 9. For 4 QLs  $\text{Bi}_2\text{Se}_3$ , the absorbance is shown in Fig. 2(a). We can see that the absorbance is high in the allowed frequency range, indicating a good frequency coverage when TI is used for photodetection. When the 3D TI is reduced to quasi-2D, the absorbance is enhanced only near the band edge, and when the photon energy increases, the absorbance drops to the 3D value of  $\mathcal{P}_{\text{gapless}} = \pi\alpha/2$ .

The gapped surface bands in the thin film TI can be classified into two classes, with one class being the time reversal partner of the other. Bands 1 and 3 are one class, the other is 2 and 4 (Fig. 2(b)). As shown in Eq. (5), near the band edge, right-handed ( $\sigma_+$ ) light couples only to 1 and 3, while left-handed ( $\sigma_-$ ) light couples only to 2 and 4. It will cause transition between the spin-down (up) valence state and the spin-up (down) conduction state. For conventional semiconductors like GaAs quantum well in [001] direction, the optical selection rules from heavy hole bands to conduction bands are as  $\sigma_{\pm} : |S\rangle \otimes |\uparrow / \downarrow\rangle \rightarrow \mp \frac{1}{\sqrt{2}} (|X\rangle \pm i|Y\rangle) \otimes |\uparrow / \downarrow\rangle$ . Here  $|S\rangle$ ,  $|X\rangle$ ,  $|Y\rangle$  and  $|\uparrow / \downarrow\rangle$  represents the orbital- and spin-part wavefunc-

tion, respectively. We can see clearly in Fig. 2(b) that the spin optical transition in the thin film TI is very different from the conventional direct-gap semiconductor such as GaAs, where the spin wavefunction remains unchanged. This unique spin optical transition selection rules make the thin film TI attractive for spintronics applications like fast switching.<sup>26</sup>

### III. TI-BASED PHOTODETECTOR

Recently, graphene has been experimentally demonstrated as a high performance THz ~ Infrared photodetector due to its zero band gap and high absorbance<sup>18</sup>. Similarly, the TI surface may also be used for such application. The figure of merit of photodetector is characterized by its SNR. Fig. 3(a) shows a typical photodetector using the TI thin film - the photoconductive resistor<sup>22</sup>. The particle and hole pairs will be generated through light absorption and the system becomes more electric conductive. Such change in conductivity can be easily measured in an electronic circuit. The SNR in such

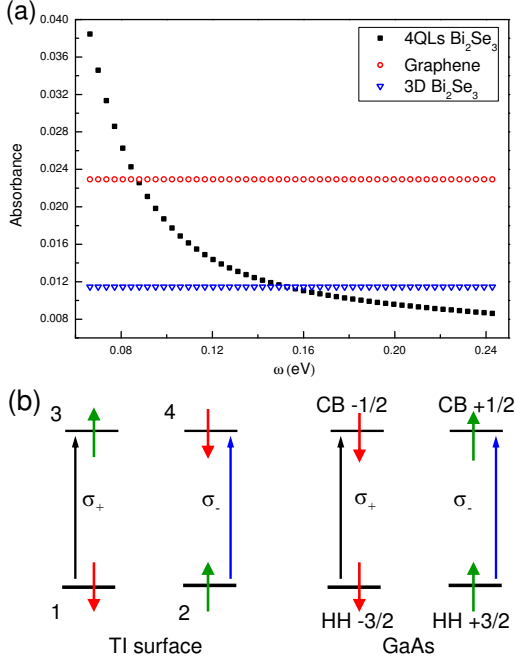


FIG. 2: **Absorption spectrum and selection rules.** (a) Absorbance for graphene, 3D and 2D TI surface bands. (b) Comparison of spin optical selection rules in GaAs and TI surface bands. The up and down arrow denotes the spin up and spin down, respectively. CB and HH denotes the conduction bands and heavy hole bands in GaAs.

system is defined by  $\text{SNR} = I_{\text{ph}}/\sigma_{I_n}$ , where  $I_{\text{ph}}$  is the photocurrent and  $\sigma_{I_n}$  is standard deviation of the noise current whose major source is the thermal noise (Johnson noise) at finite temperature  $T$  when the voltage bias  $V \ll k_B T/q^{27,28}$ .  $I_{\text{ph}} = 2q\eta PS/E_{\text{ph}}$ , here a factor of 2 represents the electron-hole pair,  $q$  is the electron charge,  $\eta$  is the quantum efficiency,  $P$  is the incident light power density,  $S$  is the detecting area and  $E_{\text{ph}}$  is the incident photon energy.  $\sigma_{I_n} = \sqrt{4k_B T \Delta f / R}$ , whereas  $\Delta f$  is the bandwidth of the detector, inversely proportional to its integration time and  $R$  is the resistance. Thus the performance of a photodetector rely on the intrinsic properties of the photodetecting material, for  $\eta$  is determined by the absorbance and  $R$  is determined by the resistivity  $\rho$ . The higher absorbance and the larger resistivity (larger band gap) the material have, the better it is to be used as a photodetector. A detailed calculation of the SNR of TI photodetectors is provided in the supplementary file<sup>29</sup>. Due to the high absorbance, 3D TI can also be used as a high performance THz ~ Infrared (0 ~ 0.3eV) photodetector, whose SNR is comparable than the commercially used bulk  $\text{Hg}_{1-x}\text{Cd}_x\text{Te}$  (Fig. 3(b)). In particular, this full spectrum can be covered by a single 3D TI detector, while for  $\text{Hg}_{1-x}\text{Cd}_x\text{Te}$ , multiple structures each covering a segment of the bandwidth by tuning the fraction  $x$  (and then band gap) have to be used, to maintain high performance, which brings much more complexities in fabrication. Moreover, the resistivity  $\rho$  can be greatly enhanced when surface opens a gap with the thickness of thin film less than several QLs. Indeed, the SNR can be improved to be about 15 times

better than  $\text{Hg}_{1-x}\text{Cd}_x\text{Te}$  (Fig. 3(b)). Besides this, the band gap of such quasi-2D system are tunable form 5meV to 0.25eV by varying its thickness<sup>9</sup> (Fig. 3(b)) where the high energy cut-off is 0.6eV here due to the confinement of bulk bands<sup>9</sup>. Photodetectors made from the  $\text{Bi}_2\text{Se}_3$  family of TIs are potentially easier to manufacture and can overcome the limitations of  $\text{Hg}_{1-x}\text{Cd}_x\text{Te}$ .

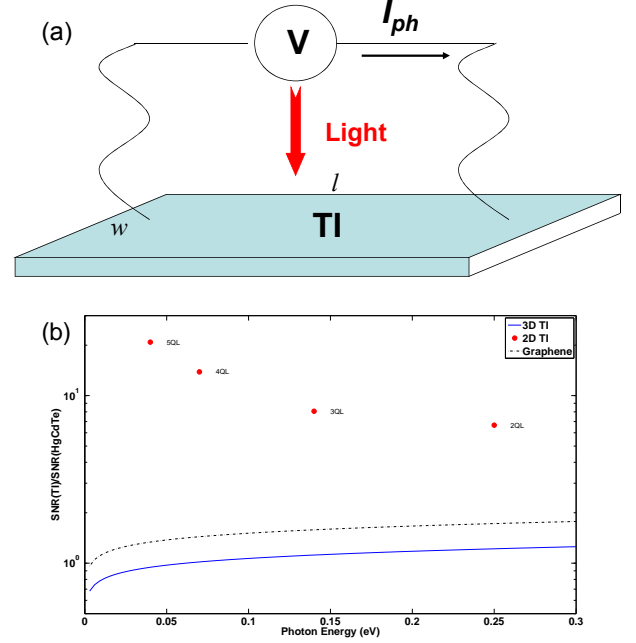


FIG. 3: **Photodetector device.** (a) Schematics of a typical photoresistor. (b) The SNR of 3D TI in full spectrum (blue line), graphene (dashed line) and 2D TI at the band edge (red point) comparing with bulk  $\text{Hg}_{1-x}\text{Cd}_x\text{Te}$ .

#### IV. CONCLUSION AND OUTLOOK

In summary, we discussed in this paper the fine structure constant defined high optical absorption of TI and its unique selection rules. Broadband and high performance photodetectors based on TI are proposed. They may find a wide range of photonic applications including thermal detection, high-speed optical communications, interconnects, terahertz detection, imaging, remote sensing, surveillance and spectroscopy<sup>18</sup>. In addition to photodetection, TI may also be used in future for other optoelectronic devices, such as terahertz laser<sup>30</sup>, waveguide<sup>31</sup>, plasmon based radiation generation and detection<sup>32</sup> and transparent electrode<sup>33</sup> etc. in analogue to graphene.

#### Acknowledgments

We wish to thank S. Raghu, J. Maciejko, S. B. Chung, R. D. Li and B. F. Zhu for insightful discussions. J.W. acknowledge

the support from NSF of China (Grant No.10774086), and the Program of Basic Research Development of China (Grant No.

2006CB921500).

- 
- <sup>1</sup> X. L. Qi and S. C. Zhang, *Phys. Today* **63**, 33 (2010).
- <sup>2</sup> B. A. Bernevig, T. L. Hughes, and S.C. Zhang, *Science* **314**, 1757 (2006).
- <sup>3</sup> M. König, S. Wiedmann, C. Brüne, A. Roth, H. Buhmann, L. Molenkamp, X.-L. Qi, and S.-C. Zhang, *Science* **318**, 766 (2007).
- <sup>4</sup> L. Fu and C. L. Kane, *Phys. Rev. B* **76**, 045302 (2007).
- <sup>5</sup> D. Hsieh, D. Qian, L. Wray, Y. Xia, Y. S. Hor, R. J. Cava, and M. Z. Hasan, *Nature* **452**, 970 (2008).
- <sup>6</sup> H. Zhang, C.-X. Liu, X.-L. Qi, X. Dai, Z. Fang, and S.-C. Zhang, *Nat. Phys.* **5**, 438 (2009).
- <sup>7</sup> Y. Xia, D. Qian, D. Hsieh, L.Wray, A. Pal, H. Lin, A. Bansil, D. Grauer, Y. S. Hor, R. J. Cava, et al., *Nat. Phys.* **5**, 398 (2009).
- <sup>8</sup> Y. L. Chen, J. G. Analytis, J. H. Chu, Z. K. Liu, S. K. Mo, X. L. Qi, H. J. Zhang, D. H. Lu, X. Dai, Z. Fang, et al., *Science* **325** (2009).
- <sup>9</sup> Y. Zhang, K. He, C.-Z. Chang, C.-L. Song, L. Wang, X. Chen, J. Jia, Z. Fang, X. Dai, W.-Y. Shan, et al., *Nat. Phys.* **6**, 584 (2010).
- <sup>10</sup> Y.-Y. Li, G. Wang, X.-G. Zhu, M.-H. Liu, C. Ye, X. Chen, Y.-Y. Wang, K. He, L.-L. Wang, X.-C. Ma, et al., *Adv. Mat.* **22**, 4002 (2010).
- <sup>11</sup> H. Li, Z. Wang, X. Kan, X. Guo, and M. Xie, *New J. Phys.* **12**, 103038 (2010).
- <sup>12</sup> D. Kong, J. C. Randel, H.-L. Peng, J. J. Cha, S. Meister, K. Lai, Y. Chen, Z.-X. Shen, H. C. Manoharan, and Y. Cui, *Nano Lett.* **10**(1), 329 (2010).
- <sup>13</sup> D. Kong, W. Dang, J. J. Cha, H. Li, S. Meister, H. Peng, Z. Liu, and Y. Cui, *Nano Lett.* **10**(6), 2245 (2010).
- <sup>14</sup> J. Linder, T. Yokoyama, and A. Sudbø, *Phys. Rev. B* **80**, 205401 (2009).
- <sup>15</sup> C.-X. Liu, H.-J. Zhang, B.-H. Yan, X.-L. Qi, T. Frauenheim, X. Dai, Z. Fang, and S.-C. Zhang, *Phys. Rev. B* **81**, 041307 (2010).
- <sup>16</sup> K. S. Novoselov, A. K. Geim, S. V. Morozov, D. Jiang, M. I. Katsnelson, I. V. Grigorieva, S. V. Dubonos, and A. A. Firsov, *Nature* **438**, 197 (2005).
- <sup>17</sup> R. R. Nair, P. Blake, A. N. Grigorenko, K. S. Novoselov, T. J. Booth, T. Stauber, N. M. R. Peres, and A. K. Geim, *Science* **320**, 1308 (2008).
- <sup>18</sup> F. Xia, T. Mueller, Y. ming Lin, A. Valdes-Garcia, and P. Avouris, *Nat. Nanotech.* **4**, 839 (2009).
- <sup>19</sup> A. H. C. Neto, F. Guinea, N. M. R. Peres, K. S. Novoselov, and A. K. Geim, *Rev. Mod. Phys.* **81**, 109 (2009).
- <sup>20</sup> H.-Z. Lu, W.-Y. Shan, W. Yao, Q. Niu, and S.-Q. Shen, *Phys. Rev. B* **81**, 115407 (2010).
- <sup>21</sup> R. Dornhaus and G. Nimtz, *Narrow Gap Semiconductors* (Springer Tracts in Modern Physics **98**, 1983).
- <sup>22</sup> H. P. K.K., *Characteristics and use of infrared detectors* (Online, 2004).
- <sup>23</sup> A. Rogalski, *J. Appl. Phys.* **93**, 4355 (2003).
- <sup>24</sup> V. Ryzhii, V. Mitin, M. Ryzhii, N. Ryabova, and T. Otsuji, *Appl. Phys. Exp.* **1**, 063002 (2008).
- <sup>25</sup> C.-X. Liu, X.-L. Qi, H.-J. Zhang, X. Dai, Z. Fang, and S.-C. Zhang, *Phys. Rev. B* **82**, 045122 (2010).
- <sup>26</sup> Y. Nishikawa, A. Tackeuchi, S. Nakamura, S. Muto, and N. Yokoyama, *Appl. Phys. Lett.* **66**, 839 (1995).
- <sup>27</sup> L. Callegaro, *Am. J. Phys.* **74**, 438 (2006).
- <sup>28</sup> <http://optical-technologies.info/p=62> (2008).
- <sup>29</sup> See EPAPS Document No. [number will be inserted by publisher] for detailed calculation of SNR of TI photodetectors in comparison with HgCdTe photodetectors. For more information on EPAPS, see <http://www.aip.org/pubservs/epaps.html>.
- <sup>30</sup> A. A. Dubinov, V. Y. Aleshkin, M. Ryzhii, T. Otsuji, and V. Ryzhii, *Appl. Phys. Express* **2**, 092301 (2009).
- <sup>31</sup> S. A. Mikhailov and K. Ziegler, *Phys. Rev. Lett.* **99**, 016803 (2007).
- <sup>32</sup> V. Ryzhii, *Jpn. J. Appl. Phys.* **45**, L923 (2006).
- <sup>33</sup> K. S. Kim, *Nature* **457**, 706 (2009).